Proceedings of the
International Conference on Mechanical Engineering 2011
(ICME2011) 18-20 December 2011, Dhaka, Bangladesh

ICME11-TH-024

SOOT FORMATION IN DIFFUSION FLAME UNDER MICROGRAVITY CONDITIONS

Arup Jyoti Bhowal

Department of Mechanical Engineering, Heritage Institute of Technology, Kolkata, India

ABSTRACT

Soot is one of the most important carcinogenic nanoparticles generated due to the combustion of hydrocarbon fuels. The laminar confined axisymetric methane-air diffusion flame was simulated numerically at reduced gravity levels. The flame height is found to decrease at microgravity level. Soot is limited to a very small region both in radial as well as axial directions. At axial heights of 6 cm and 10 cm, occurrence of soot is markedly increased at lower gravity levels of 0.25 G and 0.10 G. The centre line velocity and also the velocity in the central core are found to be reduced with the decrease of gravity levels. Hence the residence time of the gas mixture in the high temperature zone is increased. This creates a favorable condition for soot information and more soot is observed at lower gravity levels.

Keywords: Microgravity, Diffusion Flame, Soot, Conservation Equations, Finite Difference, Residence Time.

1. INTRODUCTION

The effects of gravity are sometimes undesirable in understanding certain physical, chemical or biological phenomena or studying the complex interaction of different forces involved in a process. Now-a-days, the study of combustion under microgravity condition has extended the understanding of combustion science by providing gravity-free means to unravel important physical and chemical processes, boosted by space exploration mission. There are substantial differences between normal gravity and microgravity flames. Decreasing buoyancy effect causes changes on shape, size, colour, and distribution of emission species and other main characteristics of flame. Microgravity combustion research contributes to understanding of spacecraft fire safety and diverse aspects of combustion physics.

Laminar gas jet diffusion flames are fundamental to combustion and it is one of the most commonly used flames in practical combustion chambers like gas turbine combustors, internal combustion engines and industrial furnaces. Diffusion flames are generally free from the problems associated with stability, auto-ignition, flashback etc. But, unfortunately, soot formation in practical hydrocarbon based diffusion flames has become a matter of concern over the last few decades because of its poor environmental effect. The amount of soot formed depends on the type of fuel, type of flame and other physical parameters such as temperature and residence time.

Edelman et al. [1] and Sunderland et al. [2] investigated the flame shape under microgravity conditions obtained in the NASA Lewis 2.2-s drop tower. Yuan et al. [3] demonstrated that a spherically symmetric flame configuration can be established in a microgravity environment. Papac et al. [4] created a microbuoyant condition in an earth-based laboratory to facilitate a large range of diagnostics on microgravity flames. Jia et al. [5] published a paper on numerical simulation of an enclosed laminar jet diffusion flame in microgravity environment.

Several semi-empirical soot models are available in the literature. Smith [6] proposed a soot model that assumed particle inception entirely due to physical nucleation. Kennedy et al. [7] used a one-equation model for the conservation of soot volume fraction to describe the soot formation and oxidation in an ethylene-air laminar diffusion flame. Syed et al.[8] and Moss et al. [9] used two equation models for soot volume fraction and number density in laminar diffusion flames with different fuels. Syed et al. [8] considered surface growth to be a function of the aerosol surface area, while Moss et al. [9] took it to be dependent on number density. Smooke et al. [10] developed a detailed soot growth model for an axisymmetric, laminar, coflow diffusion flame by coupling the equations of particle production and the flow and gaseous species conservation equations. They

also reported their experimental results for an overventilated, axisymmetric, coflowing atmospheric laminar methane-air diffusion flame under normal gravity conditions.

Ito et al. [11] conducted experiment to investigate the behavior of soot particles in diffusion flames under microgravity conditions using a 490-m drop shaft (10-s microgravity duration) in Hokkaido, Japan. The diameter of the agglomerated particles was 200 to 500 times as large as those generated under normal gravity. Charest et al. [12] studied the effects of pressure and gravity on the sooting characteristics and flame structure of coflow methane–air laminar diffusion flames. They observed that zero-gravity flames generally have lower temperatures, broader soot-containing zones, and higher soot volume fractions than normal gravity flames at the same pressure.

2. MATHEMATICAL MODEL

In the present work a confined axisymmetric laminar diffusion flame has been simulated under different microgravity conditions.

2.1 Physical Model

The combustion system considered in this work is the laminar diffusion flame in a confined physical environment with co-flowing fuel and air (oxidizer) streams. Two concentric vertical tubes comprise the burner. The fuel is admitted as a central jet through the inner tube and air as a co-flowing annular jet through the outer tube as shown in Fig. 1 The inner fuel tube diameter is 12.7 mm and the outer tube diameter is 50.4 mm. A cylindrical shield of diameter 50.4 mm defines an impervious outer boundary (wall) of the axisymmetric system. The fuel is considered here to be methane gas (CH_4). The numerical grid structure has also been shown in figure 1.

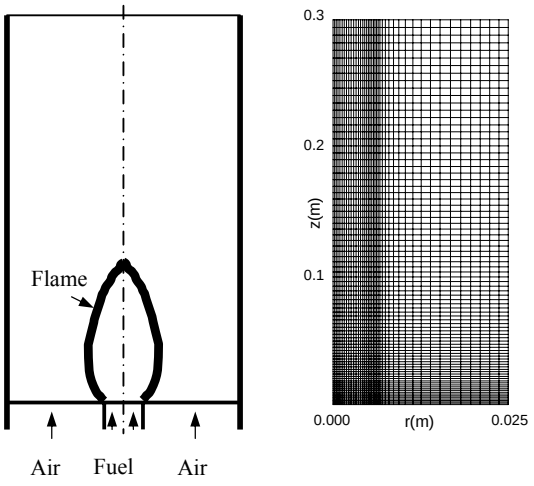

Fig.1. Physical model of the flame and grid structure

2.2. Numerical Model and Governing Equations

The numerical; model is based on solving the governing equations for reacting flow and the soot mass conservation equations with appropriate boundary conditions. The reaction between the fuel and oxidizer proceeds through two-step irreversible chemical reactions. The flow is vertical through the reaction space and the gravity effect is included in the momentum equation. A variable property formulation has been made for the transport and thermodynamic properties. The gravity level is varied by changing the values of acceleration due to gravity in the axial momentum equation.

The conservation equations considered here for mass and momentum, species concentration and energy in the cylindrical co-ordinates are as follows

Conservation of mass:

$$\frac{\partial \rho}{\partial t}+\frac{1}{r}\frac{\partial}{\partial r}\left(r\rho v_r\right)+\frac{\partial}{\partial z}\left(\rho v_z\right)=0 \tag{1}$$

Conservation of radial momentum:

$$\frac{\partial}{\partial t}\left(\rho v_r\right)+\frac{1}{r}\frac{\partial}{\partial r}\left(r\rho v_r^2\right)+\frac{\partial}{\partial z}\left(\rho v_r v_z\right)=-\frac{\partial p}{\partial r}+\frac{2}{r}\frac{\partial}{\partial r}\left(r\mu\frac{\partial v_r}{\partial r}\right)-\frac{2}{r}\mu\frac{v_r}{r^2}+\frac{\partial}{\partial z}\left\{\mu\left(\frac{\partial v_z}{\partial r}+\frac{\partial v_r}{\partial z}\right)\right\}-\frac{2}{3}\frac{\partial}{\partial r}\left\{\mu\left(\frac{\partial v_r}{\partial r}+\frac{v_r}{r}+\frac{\partial v_z}{\partial z}\right)\right\} \tag{2}$$

Conservation of axial momentum:

$$\frac{\partial}{\partial t}\left(\rho v_z\right)+\frac{1}{r}\frac{\partial}{\partial r}\left(r\rho v_r v_z\right)+\frac{\partial}{\partial z}\left(\rho v_z^2\right)=-\frac{\partial p}{\partial z}+\frac{1}{r}\frac{\partial}{\partial r}\left\{r\mu\left(\frac{\partial v_z}{\partial r}+\frac{\partial v_r}{\partial z}\right)\right\}+2\frac{\partial}{\partial z}\left(\mu\frac{\partial v_z}{\partial z}\right)-\frac{2}{3}\frac{\partial}{\partial z}\left\{\mu\left(\frac{\partial v_r}{\partial r}+\frac{v_r}{r}+\frac{\partial v_z}{\partial z}\right)\right\}+\rho g \tag{3}$$

Conservation of species:

$$\frac{\partial}{\partial t}\left(\rho C_j\right)+\frac{1}{r}\frac{\partial}{\partial r}\left(r\rho v_r C_j\right)+\frac{\partial}{\partial z}\left(\rho v_z C_j\right)=\frac{1}{r}\frac{\partial}{\partial r}\left(r\rho D_{jm}\frac{\partial C_j}{\partial r}\right)+\frac{\partial}{\partial z}\left(\rho D_{jm}\frac{\partial C_j}{\partial z}\right)+\dot{S}_{cj} \tag{4}$$

Conservation of energy

$$\frac{\partial}{\partial t}\left(\rho h\right)+\frac{1}{r}\frac{\partial}{\partial r}\left(r\rho v_r h\right)+\frac{\partial}{\partial z}\left(\rho v_z h\right)=\frac{1}{r}\frac{\partial}{\partial r}\left(r\frac{\lambda}{c_p}\frac{\partial h}{\partial z}\right)+\frac{1}{r}\frac{\partial}{\partial r}\left[r\frac{\lambda}{c_p}\sum_{j=1}^{n}h_j\left(Le_j^{-1}-1\right)\frac{\partial C_j}{\partial r}\right]+\frac{\partial}{\partial z}\left[\frac{\lambda}{c_p}\sum_{j=1}^{n}h_j\left(Le_j^{-1}-1\right)\frac{\partial C_j}{\partial z}\right] \tag{5}$$

where Le_j in the above equation is the local Lewis

number of the jth species defined as

$$Le_j = \frac{\lambda}{c_p}\frac{1}{\rho D_{jm}} \tag{6}$$

The specific heat c_p is a strong function of temperature and is locally calculated for each species at the respective temperature. The mixture specific heat is then calculated considering an ideal gas mixture. The temperature of the gas mixture is implicitly calculated from enthalpy) using Newton-Raphson method.

The transport of momentum, energy and species mass in the calculation of a reacting flow involve the transport coefficients like viscosity (μ), thermal conductivity (λ) and mass diffusivity (D_{jm}) for the mixture. The variations of those properties with temperature have been taken care by using suitable relations.

2.3. Soot Model

The formation of soot is modeled in the line prescribed by Syed et al. [8] and Moss et al. [9]. The soot volume fraction (f_v) and number density (n) are considered to be the important variables. Nucleation, surface growth, coagulation and oxidation effects are taken into account in the formation of the model equations. The conservation equations are formed for soot mass concentration ($\rho_s f_v$) and number density (as n/N_o) and the respective generation terms for the conservation equations are as follow

$$\frac{d}{dt}(\rho_s f_s) = \gamma(\rho_s f_s)^{2/3} n^{1/3} + \delta - \left(\frac{36\pi}{\rho_s^2}\right)^{1/3} \left(n\rho_s^2 f_v^2\right)^{1/3} \dot{\omega}_{ox} \tag{7}$$

$$\frac{d}{dt}\left(\frac{n}{N_0}\right) = \alpha - \beta\left(\frac{n}{N_0}\right)^2 \tag{8}$$

Where

$$\alpha = C_\alpha \rho^2 T^{0.5} X_c \exp\left(-\frac{T_\alpha}{T}\right)$$

$$\beta = C_\beta T^{0.5}$$

$$\gamma = C_\gamma \rho T^{0.5} X_c \exp\left(-\frac{T_\gamma}{T}\right)$$

$$\delta = C_\delta \alpha$$

In the above equations N_o is Avogadro number (6×10^{26}), ρ_s is the soot particulate density (=1800 kg/m^3), T_α and T_γ are activation temperatures for nucleation and growth, respectively, C_α, C_β, C_γ, C_δ are model constants and ρ and T are the local mixture density and temperature, respectively. The model constants and activation temperatures are taken from Syed et al. [8], for methane fuel. The specific rate of soot oxidation is calculated using the model of Lee et al. [13]. The soot oxidation model of Lee *et al.* is as follows:

$$\dot{\omega}_{ox} = 1.085\times 10^5 P_{O_2} T^{-1/2} \exp(-19778/T) \tag{9}$$

This has been accommodated as a negative source term in the soot volume fraction conservation equation.

Conservation equations for the soot mass concentration and number density are solved along with the gaseous species in the solution domain. As soot particles do not follow the molecular diffusion theory, the diffusion velocities in the soot conservation equations are replaced by the corresponding thermophoretic soot particle velocities. Therefore, the conservation equations, in general, can be expressed as:

$$\frac{\partial\varphi}{\partial t} + \frac{1}{r}\frac{\partial}{\partial r}\left(rv_r\varphi\right) + \frac{\partial}{\partial z}\left(\rho v_z \varphi\right) = \frac{1}{r}\frac{\partial}{\partial r}\left(rV_{t_r}\varphi\right) + \frac{\partial}{\partial z}\left(V_{t_z}\varphi\right) + \dot{S}_\varphi \tag{10}$$

The above equation is applicable both for the soot mass concentration ($\rho_s f_v$) and number density (n/N_o) and accordingly φ in the above equations will assume the respective variable value. The thermophoretic velocity vector (V_t) is calculated following Santoro et al. [14] as

$$V_t = \frac{3}{4(1+\pi\xi/8)T}\frac{\nu}{T}\nabla T \tag{11}$$

where the accommodation factor (ξ) has been taken as unity. The soot volume fraction is obtained from the mass concentration solution.

2.4 Boundary Conditions

Boundary conditions at the inlet are given separately for the fuel stream at the central jet and the air stream at the annular co-flow. The temperatures of both the inlet fuel and air are 300 K. The fuel flow rate is taken as 3.71×10^{-6} kg/s and the air flow rate is taken as 2.214×10^{-4} kg/s. No soot is assumed to enter with the flow through the inlet plane. Fully developed boundary conditions for the variables are considered at the outlet. Axi-symmetric condition is considered at the central axis, while at the wall a no-slip, adiabatic and impermeable boundary condition is adopted. No soot is assumed to enter into the computational zone. The thermophoretic velocities required for soot calculations are considered to be zero at the boundaries.

2.5. Solution Methodology

The gas phase conservation equations of mass, momentum, energy and species concentrations along with the conservation equations of soot mass concentration and number density are solved simultaneously, with their appropriate boundary conditions, by an explicit finite difference computing technique. The solution yields velocity, temperature, species concentration, soot volume fraction, soot number density throughout the computational domain at different times during the transient period and finally the steady state values. The numerical scheme adopted for solving

the reacting flow problem is based on a straight-forward, yet powerful algorithm called SOLA (Solution Algorithm) developed by Hirt and Cook [15].. The algorithm is based on primitive variables and the variables are defined following a staggered grid arrangement.

3. RESULTS AND DISCUSSION

An extensive grid independence test is carried out by several variations of the number of grids in either direction and a numerical mesh with 85×41 grid nodes is finally adopted. The soot model employed in the present work is calibrated against the experimental results of Smooke et al. [10] for the same burner configuration and input conditions for normal gravity condition.

The laminar confined axisymetric methane-air diffusion flame was simulated and numerical results were obtained for five gravity levels namely; 1.0 G (normal gravity), and reduced gravities of 0.75 G, 0.50 G, 0.25G, 0.10 G. The flame shape, the centreline velocity, the centreline temperature and soot volume fraction distribution along with centerline soot volume have been presented for these five gravity levels.

3.1 Flame Height

Figure 2(a) to figure 2(e) show the shape of flame front for five gravity levels namely, of 1.0 G, 0.75 G, 0.50 G, 0.25 G and 0.10 G. It may be seen from the figure 2(a) that the flame height is around 12 cm for gravity level of 1.0 G. It is further observed that the flame height reduces progressively as one goes for lower gravity levels with the flame height becoming around 10 cm for gravity level of 0.10 G, as shown in figure 2(b) to figure 2(e). The flame also flattens out in radial direction for lower gravity levels. This is very prominently observed in the bulge of the flame for 0.10 G. This is because of the lower buoyancy force and also lower recirculation of ambient air at lower gravity levels. This gives rise to a near spherical flame shape as gravity level deceases.

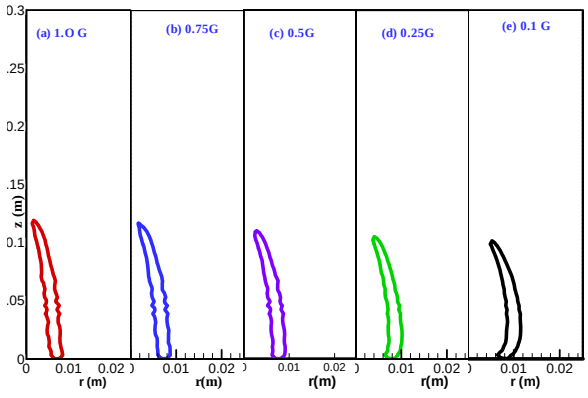

Fig 2 Shape of the flame for five different gravity levels : (a) 1.0 G, (b) 0.75 G, (c) 0.50 G, (d) 0.25 G and (e) 0.10 G

3.2 Centre Line Velocity and Temperature

Figure 3 shows the distributions of centerline velocity against the axial height for the five different gravity levels as already mentioned. It is observed that the centerline velocity continuously increases along the axis for higher gravity levels of 1.0 G, 0.75 G and 0.50 G; however the rate of increase slows down as one goes for higher axial heights. For lower gravity levels of 0.25 G, and 0.10 G, the values increase only up to an axial height of around 8 cm then decreases slightly for 0.25 G gravity level. However for 0.10 G gravity level the value remains almost stationary after reaching the peak value at a height of 12 cm. The general trend shows lower values for lower gravity levels because of lower buoyancy forces.

The centerline temperature distribution gives the indication of the flame height and is shown in Fig. 4. The distribution curves are almost overlapping one another indicating that there is only little variation with variation of gravity levels. However, the highest temperature point on the axis for 1.0 G is 12 cm and a little lower for other gravity levels indicating that the flame height decreases marginally as one goes for lower gravity levels.

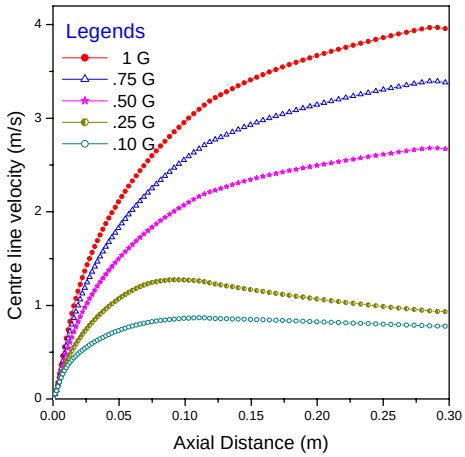

Fig 3 Centre line velocity for different gravity levels

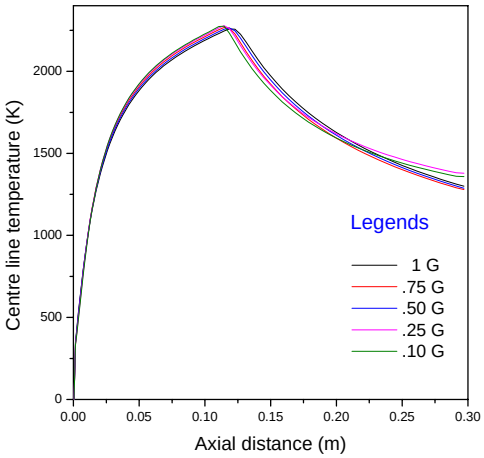

Fig 4 Centre line temperature for different gravity levels

3.3 Soot Volume Fraction Distributions

Figure 5(a) to 5(e) show the soot volume fraction contours in the r-z plane for the five gravity levels namely, of 1.0 G, 0.75 G, 0.50 G, 0.25 G and 0.10 G. It is observed that soot forming zone is limited to a narrow region – a maximum of 12 cm in the axial direction and a maximum of around 0.7 cm in the radial direction for the gravity levels considered in the present numerical experiment. The maximum soot concentration at 1.0 G gravity level is found to be 60×10^{-8}. The soot concentration is also seen to be increasing progressively as one goes for lower gravity levels. Of course, at gravity levels of 0.25 G and 0.10 G, there is an increase in order of magnitude of the soot volume fraction. The shape of the soot laden zone becomes flatter i.e. it extends in the radial direction and compresses in the axial direction.

3.4 Radial Distribution of Soot Volume

Figure 6(a) and 6(b) show the radial distributions of soot volume fraction for two axial heights, namely, 6 cm and 10 cm respectively above the burner tip for five gravity levels of 1.0 G, 0.75 G, 0.50 G, 0.25 G, and 0.10 G. At a low height of 2 cm soot is very negligible. Again beyond 10 cm height, there is practically no occurrence of soot at all because beyond this height soot is oxidized because of high temperature. At heights 6 cm and 10 cm, occurrence of soot is markedly increased at lower gravity levels of 0.25G and 0.10G. Also the soot laden zone increases in the radial direction because of flattened temperature distribution in these two gravity levels. Lower gravity levels essentially mean lower velocity and hence more residence time for soot formation.

It may be pointed out here that there is hardly any occurrence of soot at higher heights of 12 cm, 16 cm and 30 cm. They have, therefore, not been shown. A very careful observation reveals that maximum soot occurs immediately below the flame tip and inside the inner core of the primary flame.

3.5 Centre Line soot distribution

Figure 7 shows the centreline soot volume fraction distribution for the five different gravity levels taken up in the present numerical experiment. It is seen from the plot that the soot laden zone on the axis is restricted between 0.05 – 0.12 m. It is also observed that soot formation on the centerline increases with the fall in gravity level from 1.0 G to 0.10 G because of lower centerline velocity and hence more residence time.

4. CONCLUSIONS

A numerical experimentation has been performed on a laminar confined axisymetric methane-air diffusion flame under microgravity levels and results were compared with those under normal gravity. The flame height is found to be around 12 cm for normal gravity and flame height reduces with the decrease of gravity levels and it becomes approximately 10 cm for gravity level of 0.10 G (microgravity). The flame also flattens out in radial direction for lower gravity levels. This gives rise to a near spherical flame shape as gravity level deceases. The centre line velocity decreases with the decrease in gravity levels. The centre line temperature remains almost the same at different gravity levels. The soot formation in general increases with the lowering of gravity levels. In fact, there is a change in order of magnitude of soot volume fraction. Soot laden zone also extends in the radial direction with the decrease of gravity levels. Maximum soot occurs immediately below the flame tip and inside the inner core of the primary flam

5. REFERENCES

1. Edelman R. B. and Bahadori M.Y., 1986, “Effects of buoyancy on gas-jet diffusion flames: Experiment and theory”, Acta Astronautica, 13 :681–688
2. Sunderland P. B., Mendelson B. J., Yuan Z.-G. and Urban D. L., 1999, “Shapes Of Buoyant and Nonbuoyant Laminar Jet Diffusion Flames”, Combustion and Flame, 116 : 376–386
3. Yuan Z. G., Hegde U. and Faeth G. M., 2001, “Effects of Electric Fields on Non-buoyant Spherical Diffusion Flames”, Combustion and Flame, 124 : 712–716
4. Papac M.J., Dunn-Rankin D., Stipe C.B. and Lucas D., 2003, “N2 CARS Coherent Anti-Stokes Raman Spectroscopy) Thermometry and O2 LIF Concentration Measurements in a Flame under Electrically induced Microbuoyancy”, Combustion and Flame, 133 : 241–254
5. Jia K., Venuturumilli R., Ryan B.J. and Chen L.D., 2000, “Numerical simulation of an enclosed laminar jet diffusion flame in microgravity environment: comparison with elf data”, Proc. Sixth International Microgravity Combustion, 38th Aerospace Sciences Meeting and Exhibit, Reno, AIAA-2000-693.
6. Smith G.W., 1982, “A Simple Nucleation/Depletion Model for the Spherule Size of Particulate Carbon”, Combustion and Flame, 48 : 265 - 272
7. Kennedy I. M., Kollmann W. and Chen J. Y., 1990, “A Model for the Soot Formation in Laminar Diffusion Flame”, Combustion and Flame, 81: 73 - 85
8. Syed K.J., Stewart C.D. and Moss J.D., 1990, “Modelling Soot Formation and Thermal Radiation in Buoyant Turbulent Diffusion Flames”, *Proc. Twenty-Third Symposium (International) on Combustion*, The Combustion Institute, Pittsburgh, pp. 1533-1539.
9. Moss J.B., Stewart C.D. and Young K.J., 1995, “Modelling Soot Formation and Burnout in a High Temperature Laminar Diffusion Flame Burning Under Oxygen-enriched Conditions”, Combustion and Flame, 101 : 491 - 500
10. Smooke M.D., McEnally C.S., Pfefeerle L.D., Hall R.J. and Colket M.B., 1999, “Computational and Experimental Study of Soot Formation in a Coflow Laminar Diffusion Flame”, Combustion and Flame, vol. 117 : 117 - 139
11. Ito H., Fujita O. and Ito K., 1994, “Agglomeration of Soot Particles in Diffusion Flames under Microgravity”, Combustion and Flame, 99 :

363-370
12. Charest M. R. J., Groth C. P. T. and Gülder Ö. L., coflow methane–air diffusion flames at pressures from 1 to 60 atmospheres", Combustion and Flame, 158 : 860–875.
13. Lee K.B., Thring M.W. and Beer J.M., 1962, "On the Rate of Combustion of Soot in a Laminar Soot Flame", Combustion and Flame, 6 : 137 -145
14. Santoro R.J., Yeh T.T., Horvath J.J. and Semerjian H.G., 1987, "The Transport and Growth of Soot Particle in Laminar Diffusion Flames", Combustion Science and Technology, 53 : 89 –115
15. Hirt C.W. and Cook J.L., 1972, "Calculating Three-Dimensional Flows Around Structures and over Rough Terrain", Journal of Computational Physics,. 10 : 324 – 338

6. NOMENCLATURE

Symbol	Meaning	Unit
C_j	Concentration of j^{th} species	-
c_p	Specific heat	$J.kg^{-1}.K^{-1}$
D	Mass diffusivity	$m^2.s^{-1}$
f_v	Soot volume fraction	-
g	Acceleration due to gravity	$m.s^{-2}$
h	Enthalpy	$J.kg^{-1}$
Le =	Lewis number	-
T =	Temperature	K
v =	Velocity	$m.s^{-1}$
g =	Acceleration due to gravity	$m.s^{-2}$
μ	viscosity	$kg.m^{-1}.s^{-1}$
ρ	density	$kg.m^{-3}$
λ	Thermal conductivity	$W.m^{-1}.K^{-1}$

7. MAILING ADDRESS

Mr. Arup Jyoti Bhowal
Department of Mechanical Engineering
Heritage Institute of Technology,
Kolkata – 700107, West Bengal, INDIA.
Phone : +913324430454
FAX : +913324430455
E-mail : arupjyoti.bhowal@heritageit.edu

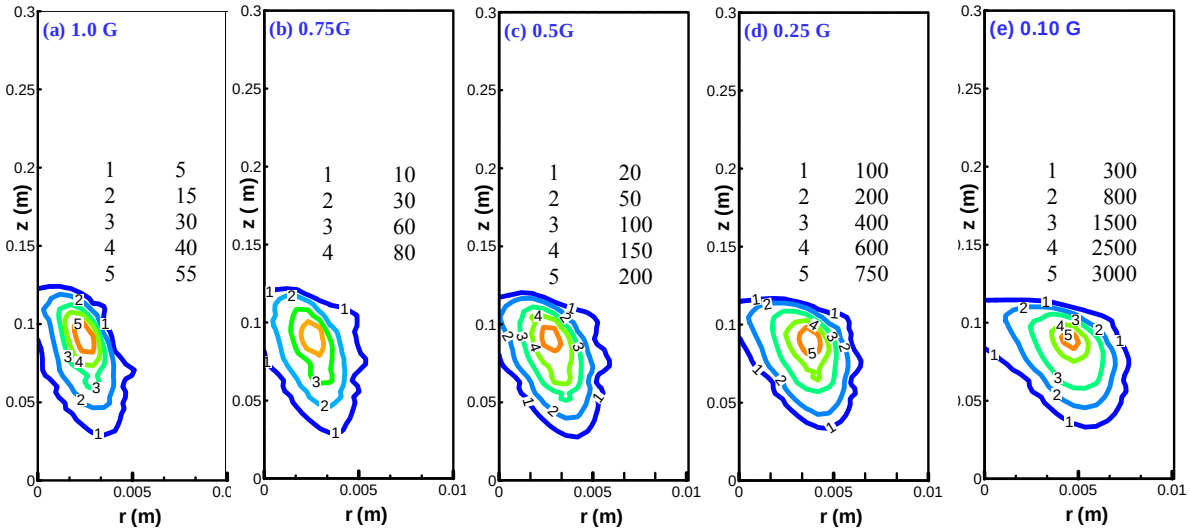

Fig 5. Soot volume fraction (f_v)isopleths for five gravity levels : (a) 1.0 G (b) 0.75 G (c) 0.50 G (d) 0.25 G and (e) 0.10 G. The values of f_v shown in the figure are the actual values multiplied by 10^8.

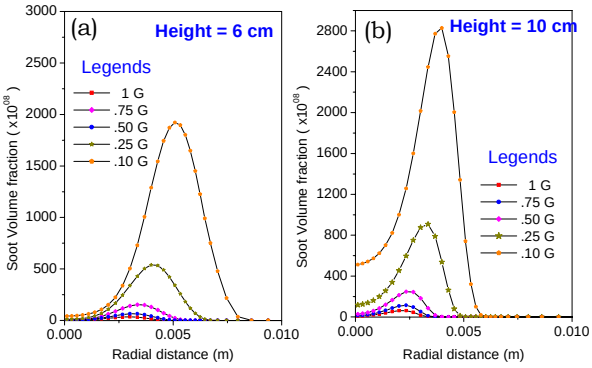

Fig 6. Radial distributions of soot volume fraction for different gravity levels at axial heights: (a) 6 (b) 10 cm

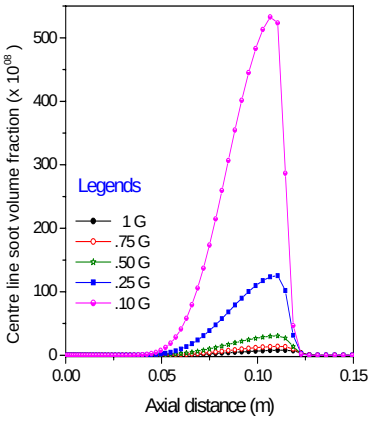

Fig 7. Centre line soot volume fraction distribution for different gravity levels